J. Cent. South Univ. (2021) 28: 3666−3680
DOI: https://doi.org/10.1007/s11771-021-4845-0

Springer

Efficient adsorption removal and adsorption mechanism of basic fuchsin by recyclable Fe_3O_4@CD magnetic microspheres

NING Jing-heng(宁静恒)[1]*, CHEN Dong-er(陈冬儿)[1], LIU Yong-le(刘永乐)[2], HUANG Shou-en(黄寿恩)[2], WANG Fa-xiang(王发祥)[2], WEI Rui(魏锐)[1], HU Qiong-can(胡琼璨)[1], WEI Jia-qian(魏佳倩)[1], SUN Chang(孙畅)[1]

1. School of Chemistry and Chemical Engineering, Changsha University of Science & Technology, Changsha 410110, China;
2. School of Food and Biological Engineering, Changsha University of Science & Technology, Changsha 410110, China

Abstract: Excessive discharge of dye wastewater has brought serious harm to human health and the environment. In this paper, a magnetic absorbent, ferroferric oxide@*β*-cyclodextrin (Fe_3O_4@CD), was prepared for the efficient adsorption removal of basic fuchsin (BF) from dye wastewater, based on the special amphiphilicity of *β*-CD and the strong magnetism of Fe_3O_4. A series of influence factors including the initial dye concentration, adsorbent dosage, temperature and pH were investigated, as well as the adsorption mechanism. The results show that Fe_3O_4@CD has the best adsorption and removal effect on BF dye at room temperature and neutral pH, when the initial concentration of dye is 25 mg/L and the adsorbent dosage is 100 mg. The adsorption behavior conforms to the pseudo-second-order kinetics and the Langmuir adsorption isotherm, and the adsorption process is spontaneously endothermic. Fe_3O_4@CD adsorbed with BF dye can be rapidly separated under an external magnetic field and then easily regenerated by HCl treatment. After 5 times of recycling, the removal rate of the prepared magnetic composite on BF dye is kept above 75%. This work will provide an economic and eco-friendly technology for the treatment of the actual dye wastewater.

Key words: Fe_3O_4@CD magnetic microspheres; adsorption removal; basic fuchsin

Cite this article as: NING Jing-heng, CHEN Dong-er, LIU Yong-le, HUANG Shou-en, WANG Fa-xiang, WEI Rui, HU Qiong-can, WEI Jia-qian, SUN Chang. Efficient adsorption removal and adsorption mechanism of basic fuchsin by recyclable Fe_3O_4@CD magnetic microspheres [J]. Journal of Central South University, 2021, 28(12): 3666−3680. DOI: https://doi.org/10.1007/s11771-021-4845-0.

1 Introduction

Basic fuchsin (BF) is a bright red water-soluble triphenyl methane derivative, widely used in printing and dyeing, paper, textile, leather and synthetic fiber industries [1, 2]. However, the aromatic structure of BF is highly toxic and may damage human organs or nervous systems [3]. The discharge of BF dye into water will seriously pollute the environment and pose a huge threat to human health [4]. Thus, it is urgent to develop efficient

Foundation item: Project(2017YFC1600306) supported by the National Key R&D Program of China; Project(21505005) supported by the National Natural Science Foundation of China; Project(2018JJ2424) supported by the Hunan Provincial Natural Science Foundation, China; Project(2019IC21) supported by the International Cooperative Project for "Double First-Class", China

Received date: 2021-01-19; **Accepted date:** 2021-10-28

Corresponding author: NING Jing-heng, PhD, Associated Professor; Tel: +86-731-85258733; E-mail: ningjingheng@126.com; ORCID: https://orcid.org/0000-0001-6983-8192

technologies for the treatment of BF dye wastewater. At present, the main purification methods of dye wastewater include adsorption [5], biodegradation [6], photodegaradation [7, 8], chemical oxidation and precipitation [9], coagulation [10] and electrochemical method [11].

Among them, the adsorption method has been extensively used due to its outstanding advantages such as simple operation, low cost, high removal efficiency and no secondary pollution [12]. AHMED et al [13] synthesized waste foundry sand coated with magnesium/iron-layered double hydroxides (WFS/MgFe-LDH) nanoparticles by a co-precipitation method, and its adsorption performance was evaluated by a set of batch tests for the sorption of Congo red dye from wastewater. SHARMA et al [14] synthesized starch/poly (alginic acid-cl-acrylamide)/Fe/Zn nanocomposite hydrogel (ST/PL(AA-cl-AAm)/Fe/Zn NCHG) by simple polymerization/co-precipitation method for photocatalytic degradation of the mixture of malachite green and fast green dye. ALBADARIN et al [15] prepared activated lignin-chitosan extruded (ALiCE) pellets by a new method involving extrusion and thermal activation, for selective adsorption of the cationic dye methylene blue (MB). However, the adsorption capacity of activated carbon, diatomite and other common adsorbents is limited, and the recovery process is complex, which requires further improvement [16, 17]. It is of great significance to develop new adsorbents with good adsorption performance as well as convenient separation and regeneration.

Magnetic nano-adsorbent has high specific surface area/volume ratio and can adsorb dye pollutants well. Due to its unique magnetic properties, this kind of adsorbent can be rapidly separated and removed with the help of an external magnetic field, so it can be easily regenerated and reused many times [18, 19]. In a word, magnetic absorbent not only simplifies the operation process, but also greatly reduces the cost, and has a very broad application prospect in wastewater treatment [20]. At present, Fe_3O_4 magnetic nanoparticles with high specific surface area have been frequently reported to be used for the adsorption and removal of dye pollutants due to their simple preparation, easy modification and low toxicity [21]. For example, FAN et al [22] prepared Fe_3O_4@MIL-100 (Fe) composite materials, which were combined with bacterial cells for adsorption and biodegradation of dyes from wastewater. JOSHI et al [23] prepared Fe_3O_4 nanoparticles loaded with activated carbon (Fe_3O_4@AC), which showed good adsorption performance for cationic dyes due to plenty of negative charges on their surface. CHATTERJEE et al [24] synthesized recyclable Fe_3O_4@BTCA with a greater surface area and charge through modifying Fe_3O_4 NPs by 1,2,4, 5-benzotetracylic acid (BTCA), which could adsorb Congo red dye well due to strong H-bond interactions between the dye molecule and BTCA. However, it is well known that Fe_3O_4 magnetic particles are prone to agglomeration and oxidation, especially corrosion under acidic conditions, which limits their application. Therefore, in order to improve the stability, dispersibility and biocompatibility, nowadays researchers still focus on the modification of Fe_3O_4 magnetic nanoparticles with various functional compounds to meet different application requirements [25, 26].

β-cyclodextrin (β-CD) has a special amphiphilic structure with hydrophobic cavity and hydrophilic outer wall, which is widely used to form host-guest complexes to improve the properties of organic guest compounds. And it can be used as a surfactant for the modification of carbon nanomaterials to improve their dispersion and stability in water [27, 28]. It has been reported that β-CD can introduce organic pollutants into its hydrophobic cavity, thereby removing them from wastewater [29, 30]. For example, TAKA et al [31] developed a new polymer nano-biosorbent with high specific surface area using nano-β-CD-polyurethane, titanium dioxide, silver nanoparticles and phosphorylated multi-walled carbon nanotubes, which could effectively adsorb trichloroethylene and Congo red dye in wastewater samples. LIU et al [32] prepared β-cyclodextrin functionalized magnetic graphene hybrid (m-GOβ-CD), and found that the introduction of β-CD greatly improved the adsorption capacity of rhodamine 6G and acid fuchsin, and β-CD showed a strong interaction with the organic dye. QU et al [33] used β-CD functionalized cellulose for simultaneous removal of atrazine and Pb (II), based on different adsorption mechanisms for atrazine (host-guest interaction) and Pb (II) (complexation and electrostatic interaction). Meanwhile, as a natural oligosaccharide, β-CD has many other merits suitable for wastewater treatment, such as cheap and

easy to obtain, non-toxic, environment-friendly and biodegradable. However, β-CD is soluble and cannot be easily separated from water for recycling [34]. Therefore, we consider immobilization of β-CD on Fe_3O_4 nanoparticles to make it be used better for the treatment of dye wastewater. Fe_3O_4 nanoparticles have excellent magnetic properties (they can be separated quickly in the external magnetic field), which overcomes the difficulty of β-CD regeneration. And the special amphiphilicity of β-CD prevents the aggregation of Fe_3O_4, which improves the stability and dispersibility of β-CD.

In this paper, ferroferric oxide@β-cyclodextrin magnetic microspheres (Fe_3O_4@CD) were prepared on the basis of our previous work [35]. As shown in Scheme 1, the magnetic adsorbent could effectively adsorb and remove BF dyes from wastewater and would have good regeneration performance. The adsorption properties of BF dyes on Fe_3O_4@CD under different conditions was studied, and the adsorption mechanisms including kinetics, isotherm models and thermodynamics were further investigated. Kinetics data accord with a pseudo-second-order kinetic model, implying that the rate-determining step is controlled by chemisorption. Isotherm data fit well with the Langmuir model of a monolayer adsorption. Thermodynamic study shows that the adsorption process is endothermic with an entropy increase, suggesting that this process is spontaneous. Meanwhile, regeneration experiments show that Fe_3O_4@CD can still have a good adsorption effect on BF after being recycled 5 times. These excellent performance of the prepared Fe_3O_4@CD magnetic adsorbent may be attributed to: 1) β-CD can adsorb BF by introducing the triphenylmethyl center of BF into its hydrophobic cavity, while Fe_3O_4 (which is rich in negative OH^- on its surface) can adsorb positive BF *via* electrostatic interactions [23], making Fe_3O_4@CD composite have a greater adsorption capacity; 2) the intrinsic magnetism of Fe_3O_4 endows the Fe_3O_4@CD composite with good regenerability, which ensures that the pollutants can be quickly and easily separated from wastewater under an external magnetic field after the adsorption is completed; 3) the unique amphiphilic structure of β-CD enables Fe_3O_4@CD magnetic microsphere to have good stability and dispersibility, which overcomes the disadvantages of Fe_3O_4 nanoparticles being easy to be oxidized and agglomerated. In a word, the

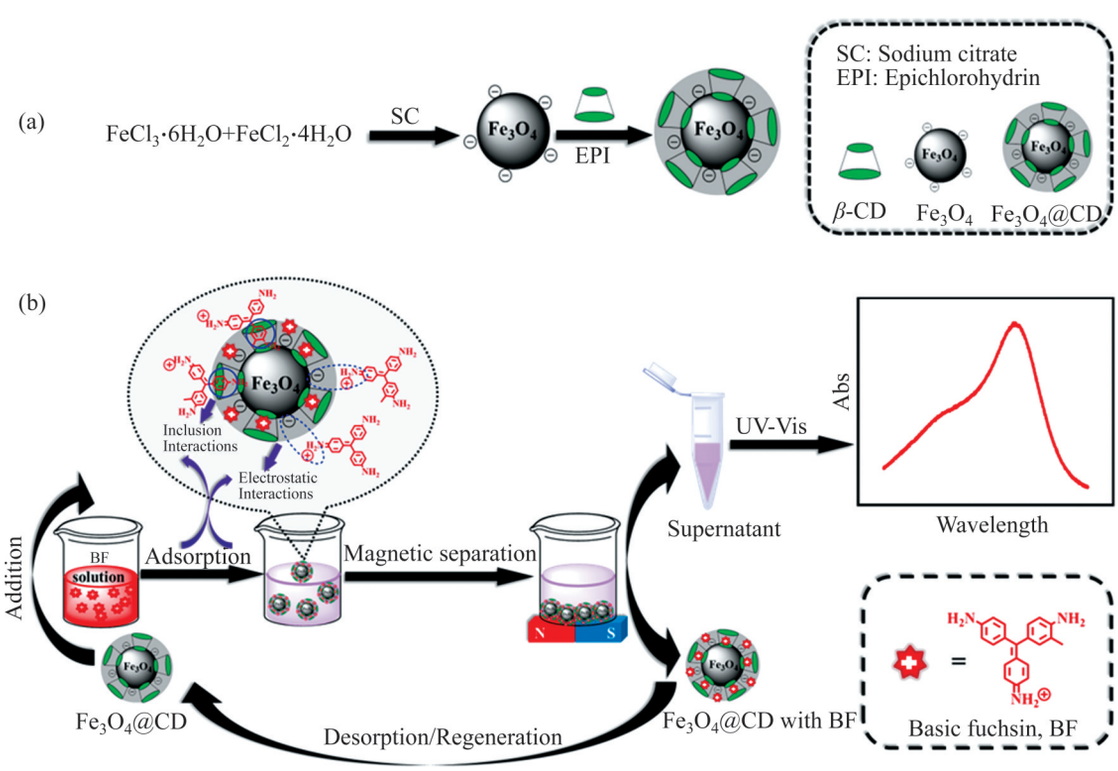

Scheme 1 Preparation of Fe_3O_4@CD magnetic microspheres (a) and adsorption removal of basic fuchsin dyes using recyclable Fe_3O_4@CD magnetic microsphere (b)

prepared Fe_3O_4@CD magnetic absorbent exhibits outstanding advantages of simplicity, high efficiency, good repeatability, low cost and strong ability to remove BF, which provides the possibility for developing new wastewater treatment technologies and exploring new application prospects.

2 Experimental

2.1 Materials

Ferric chloride hexahydrate ($FeCl_3·6H_2O$), ferrous chloride tetrahydrate ($FeCl_2·4H_2O$), hydrogen chloride (HCl), ammonium hydroxide (NH_4OH), sodium hydroxide (NaOH), basic fuchsin (BF), β-cyclodextrin (β-CD), sodium citrate (SC), methanol, Span 80 and Tween 20 were purchased from the Sinopharm Chemical Reagent Co., Ltd (Shanghai, China). Acetone was purchased from Hunan Normal University Chemical Reagent Factory (Hunan, China). Epichlorohydrin (EPI) was purchased from Hunan Huihong Reagent Co., Ltd (Hunan, China). Span 80 and Tween 20 were of chemical grade, while all the other chemicals were of analytical grade. All reagents were used as received without any further purification.

2.2 Characterization

Fourier transform infrared (FT-IR) spectrum was recorded from 4000 cm^{-1} to 400 cm^{-1} by FT-IR spectrometer (Avatar 360, Thermo Nicolet Corporation, Madison, WI, USA). X-ray diffraction (XRD) analysis was performed on X-ray diffractometer (MAX-2500, Rigaku Corporation, Tokyo, Japan). The surface morphology was characterized by the scanning electron microscope (SEM) (JEM-3010, Shimadzu Corporation, Tokyo, Japan). UV-absorbance spectrum of BF was obtained with UV-Vis spectrophotometer (TU-1901, Beijing Purkinje General Instrument Co., Ltd., Beijing, China). All pH values were accurately measured by a pH meter (Shanghai YOUKE Instrument Co., Ltd., Shanghai, China).

2.3 Preparation of Fe_3O_4@CD magnetic microspheres

The composite Fe_3O_4@CD was prepared by improving the method reported in Ref. [36]. Firstly, 4 mL of HCl solution, 0.886 g of $FeC1_3·6H_2O$ and 0.341 g of $FeC1_2·4H_2O$ were quickly added into 1 mol/L NH_4OH solution, stirring and reacting for 0.5 h under the protection of nitrogen. Then 60 mL 0.5 mol/L SC solution was added to the reaction mixture, continuing to react for 1 h. And then the reactant was precipitated with acetone, affording Fe_3O_4 magnetic nanoparticles. Finally, Fe_3O_4 particles were re-dispersed in de-ionized water by ultrasound for subsequent use. The Fe_3O_4 dispersion solution was added into NaOH solution and ultrasonicated for 20 min, then the mixture was transferred into a 250 mL three-necked flask for a water bath at a constant temperature of 30 °C. Add 6 g of β-CD into the flask and stir the mixture into a uniform black paste, then add EPI and continue to stir for 1.5 h. Add Span 80 and Tween 20 kerosene to the mixture and raise the temperature to 70 °C at the same time, continuing to react for 8 h. Finally, the mixed solution was centrifuged to remove the supernatant, and the obtained solid was successively washed with diluted HCl, methanol, distilled water and acetone, and then was dried in vacuum at 60 °C to obtain Fe_3O_4@CD magnetic microspheres.

2.4 Adsorption removal of BF by Fe_3O_4@CD magnetic microspheres

To investigate the adsorption performance of Fe_3O_4@CD magnetic microspheres, a series of experiments on the adsorption of BF by Fe_3O_4@CD magnetic microspheres were carried out. Firstly, an appropriate amount of the prepared Fe_3O_4@CD magnetic microspheres was added to 25 mL of BF solution of a certain concentration, and pH value was adjusted with HCl and NaOH solutions by pH meter. After shaking at room temperature for a few minutes, the Fe_3O_4@CD magnetic microspheres were separated under an external magnetic field. Finally, the residual amount of BF in the supernatant was determined by UV-Vis spectrophotometer at a λ_{max} of 544 nm. The removal rate (η) and the adsorption capacity (q, mg/g) of BF by Fe_3O_4@CD magnetic microspheres could be calculated according to the following Eqs. (1) and (2), respectively:

$$\eta = \frac{C_0 - C_t}{C_0} \times 100\% \quad (1)$$

$$q = \frac{(C_0 - C_t)V}{m} \quad (2)$$

wherein C_0 (mg/L) is the initial concentration of the BF dye solution; C_t (mg/L) is the concentration of the BF dye solution at time t; V (L) is the volume of the BF dye solution; and m (g) is the dosage of Fe_3O_4@CD adsorbent.

2.5 Regeneration of Fe_3O_4@CD magnetic adsorbent

To investigate the regeneration performance of the prepared Fe_3O_4@CD adsorbent, HCl solution was used to desorb BF from the adsorbent in the regeneration experiment. Firstly, 100 mg of Fe_3O_4@CD magnetic microspheres were added to 25 mL of BF solution (25 mg/L) at pH 7 and stirred at room temperature for 1 h. The removal rate of BF dye solution could be calculated according to the above-mentioned Eq. (1). Secondly, add HCl solution into the mixture and heat it to 40 °C, and then stir for a while. Thereafter, the adsorbent was separated out of the mixture by an external magnetic field, and dried in vacuum at 60 °C to get regenerated. Finally, this reproduced adsorbent was reused for the adsorption experiment once again. Such kind of recycling experiment was repeated 5 times.

3 Results and discussion

3.1 Structure of Fe_3O_4@CD magnetic microspheres

The structure, morphology and magnetic performances of the prepared Fe_3O_4@CD composites were studied by FT-IR and XRD, SEM or under an external magnetic field, respectively, as well as the spectrum of Fe_3O_4@CD adsorbed with BF to study the adsorption between them (see Figure 1). In Figure 1(a), curve a is the infrared spectrum of BF, the broad absorption peak at 3186 cm^{-1} can be attributed to the stretching vibration of —C—H on the benzene ring, the peak at 1579 cm^{-1} can be attributed to the stretching vibration of —C═C— double bond of benzene ring, and the peak at 1365 cm^{-1} can be attributed to the vibration of —C—N— single bond of aromatic amine. The infrared spectrum of β-CD (curve b) has a strong absorption peak at 3400 cm^{-1}, which can be attributed to the stretching vibration peaks of –OH. The absorption peaks at 2900 cm^{-1} and 1380 cm^{-1} can be attributed to the antisymmetric stretching vibration and symmetrical deformation vibration of —CH_2, respectively. In curve c, it can be seen that Fe_3O_4 has a characteristic absorption peak of Fe—O at 533 cm^{-1}. As for the composite Fe_3O_4@CD (curve d), the characteristic peak of —CH_2 group in β-CD at 2900 cm^{-1} and the typical peak of Fe—O group in Fe_3O_4 at 533 cm^{-1} appear at the same time, indicating the successful composition of β-CD and Fe_3O_4. Curve e is the infrared spectrum of Fe_3O_4@CD adsorbed with BF. Obviously, it can be seen at the same time all the characteristic adsorption peaks, such as peaks of —CH_2 in β-CD at both 2900 cm^{-1} and 1380 cm^{-1}, peak of —C═C— double bond in BF at 1579 cm^{-1} and the characteristic peak of Fe—O bond in Fe_3O_4 at 533 cm^{-1}. And the intensity of these characteristic absorption peaks is obviously weakened. These results show that the prepared Fe_3O_4@CD can adsorb BF dye. Figure 1(b) shows the XRD patterns of the prepared Fe_3O_4 (curve a) and Fe_3O_4@CD (curve b). In curve a, the characteristic peaks of Fe_3O_4 are located at 30.0°, 35.1°, 43.1°, 53.6°, 57.4° and 62.4°, respectively, corresponding to the (220), (311), (400), (422), (511) and (440) crystal faces of magnetite. The results indicate that the prepared Fe_3O_4 has a good crystal shape, as described in the JCPDS card (No. 88−315) [37]. In curve b, after Fe_3O_4 is modified by β-CD, a broad diffraction peak appears near 18.8°, which is the diffraction peak of β-CD [38], and the diffraction peak of Fe_3O_4 can also be observed. These results are consistent with previous literatures and the results of FT-IR spectra, confirming the successful preparation of Fe_3O_4@CD. Figure 1(c) shows SEM images of the composite. Obviously, the prepared Fe_3O_4@CD composites are spherical particles of uniform size. From the inset (a high-magnification image), it is clear that the average particle size is about 45 μm and the particle surface is quite smooth. In Figure 1(d), the left photograph shows that the prepared Fe_3O_4@CD particles have good

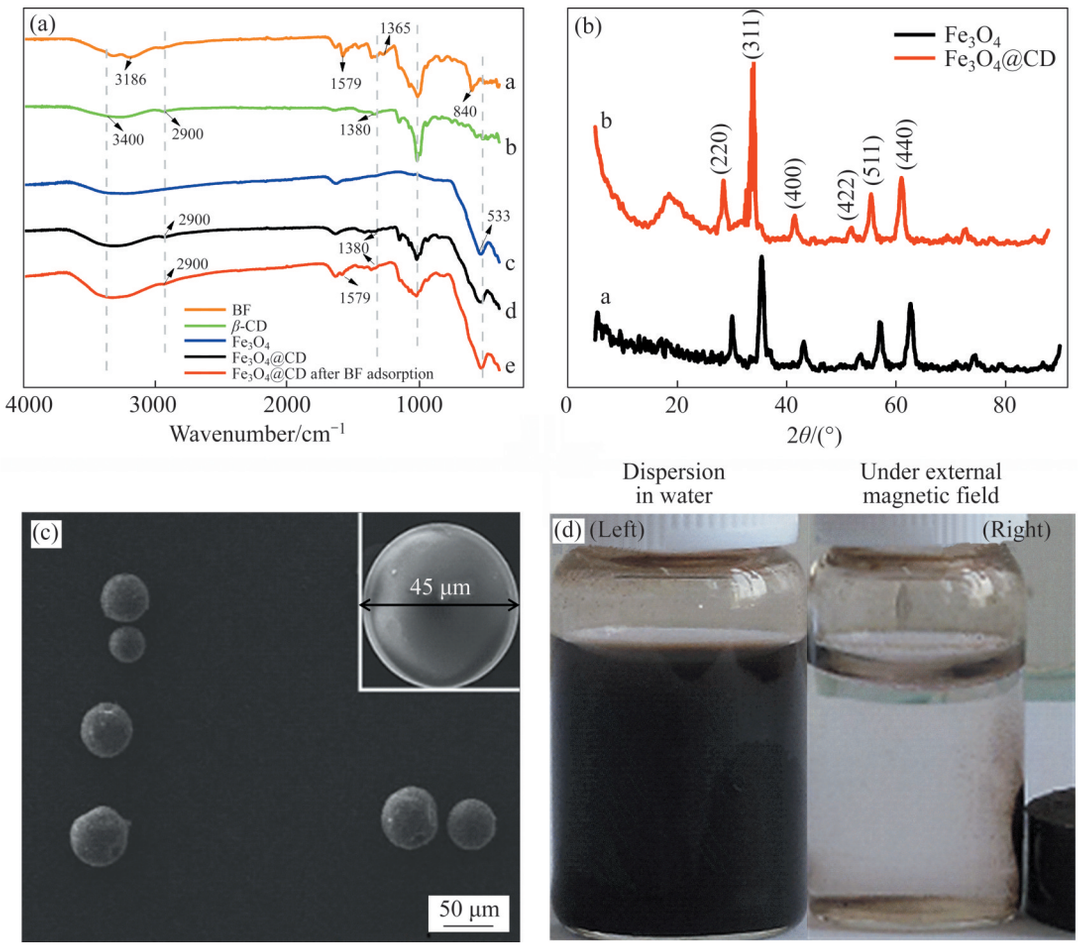

Figure 1 (a)FT-IR spectra of BF, β-CD, Fe_3O_4, Fe_3O_4@CD and Fe_3O_4@CD adsorbed with BF; (b) XRD pattern of Fe_3O_4@CD; (c) SEM images of Fe_3O_4@CD(inset: high-magnification SEM image); (d) Good dispersion of Fe_3O_4@CD particles in water (the left photograph) and easy separation of Fe_3O_4@CD microspheres under an external magnetic field (the right photograph)

dispersibility in water. Meanwhile, the right photograph shows that Fe_3O_4@CD particles can be readily separated under an external magnetic field, implying that the composite is paramagnetic. This is very important for subsequent regeneration studies because only strong enough magnetism can ensure rapid separation and efficient recovery of the absorbent, as we expected.

3.2 Adsorption effect of BF by Fe_3O_4@CD magnetic microspheres and condition optimization for adsorption

3.2.1 Optimization of BF initial concentration

The influence of the initial concentration of BF dye (from 5 mg/L to 25 mg/L) on the adsorption effect was investigated, with 100 mg of Fe_3O_4@CD under pH 7 at room temperature. The results are shown in Figure 2(a). Obviously, with the increase of BF initial concentration, the adsorption capacity of Fe_3O_4@CD toward BF dye (q) increases but the dye removal rate decreases. The increase of q may be because with the increase of BF concentration, the effective collision between dye molecules and Fe_3O_4@CD adsorbent is more frequent, making the adsorption process easier. However, at a higher BF concentration, the active sites of the fixed dosage of Fe_3O_4@CD adsorbent become insufficient, leading to relatively fewer dye molecules attracted by Fe_3O_4@CD, which results in a decrease in the dye removal rate. As shown in Figure 2(a), when BF initial concentration increases from 5 mg/L to 25 mg/L, the adsorption capacity increases from 6.6 mg/g to 31.8 mg/g, and the BF removal rate decreases from 99.8% to 95.4%. Therefore, considering a large adsorption capacity with a

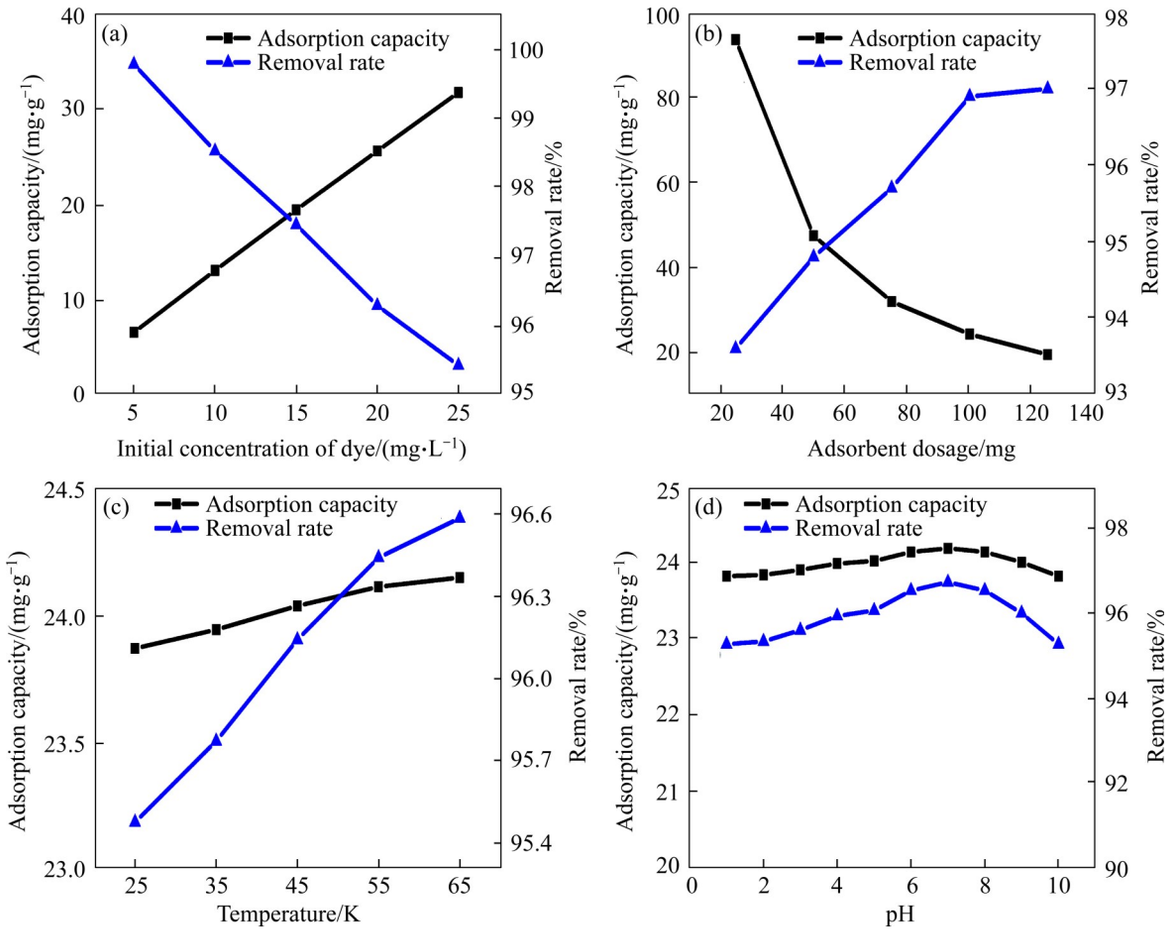

Figure 2 (a) Influence of initial concentration of BF dye (from 5 mg/L to 25 mg/L) on the adsorption effect (Fe_3O_4@CD 100 mg; room temperature, neutral pH); (b) Influence of Fe_3O_4@CD dosage (from 25 mg to 125 mg) on the adsorption effect (BF initial concentration 25 mg/L; room temperature, neutral pH); (c) Influence of temperature (from 298.15 K to 338.15 K) on the adsorption effect (BF initial concentration 25 mg/L, Fe_3O_4@CD 100 mg, neutral pH); (d) Influence of pH (from 1 to 10) on the adsorption effect (BF initial concentration 25 mg/L, Fe_3O_4@CD 100 mg, room temperature)

remove rate not less than 95%, the optimal initial BF concentration is selected as 25 mg/L for subsequent tests.

3.2.2 Optimization of adsorbent dosage

Since both the effective surface area and the active sites of the adsorbent can affect the adsorption of dyes, it is necessary to carry out experiments related to the amount of absorbent. The influence of Fe_3O_4@CD dosage on the adsorption effect was studied based on an absorbent dosage ranging from 25 mg to 125 mg, with a BF initial concentration of 25 mg/L under pH 7 at room temperature. The results are shown in Figure 2(b). Apparently, when the dosage of Fe_3O_4@CD increases from 25 mg to 125 mg, the adsorption capacity, q, drops down from 93.6 mg/g to 19.4 mg/g, while the BF dye removal rate goes up from 93.6% to 97%. It is worth noting that the increase of the removal rate tends to be slow when Fe_3O_4@CD dosage increases from 100 mg to 125 mg. This phenomenon may be caused by the increase of Fe_3O_4@CD dosage, there are more active sites to attract dye molecules, thus improving the BF removal rate. However, when the adsorbent dosage increases to a certain amount, the active sites will become enough for dye molecules. So the higher the adsorbent dosage is, the more the active sites remain vacant, and the slower the removal rate increases. Therefore, 100 mg of Fe_3O_4@CD is selected as the best adsorbent dosage for BF dye adsorption.

3.2.3 Optimization of temperature

Temperature plays an important role in the adsorption process. The influence of temperature on

the adsorption effect was studied from 25 °C to 65 °C (from 298.15 K to 338.15 K) at pH 7, under a BF initial concentration of 25 mg/L and 100 mg of Fe_3O_4@CD. As shown in Figure 2(c), with the increase of temperature, both the adsorption capacity and removal rate increase. It is worth noting that even at room temperature (25 °C), q can reach 23.8 mg/g, and the removal rate is as high as 95.5%. These results indicate that the prepared Fe_3O_4@CD adsorbent has excellent adsorption performance for BF at different temperatures. This implies that the adsorption of BF by Fe_3O_4@CD is an endothermic process. When the temperature rises, the movement speed of BF dye molecules is accelerated, that is to say, the effective collision between BF and Fe_3O_4@CD increases, making more BF dye molecules attracted onto the surface of Fe_3O_4@CD. In order to save cost and energy, 25 °C is chosen as the most appropriate temperature for the adsorption removal of BF by Fe_3O_4@CD.

3.2.4 Optimization of pH

The pH value of the solution is crucial in the adsorption process because it affects the ionization of the dye molecules and the surface charge of the adsorbent. Thus, the influence of the pH from 1 to 10 was investigated at 25 °C, under a BF initial concentration of 25 mg/L and 100 mg of Fe_3O_4@CD. As shown in Figure 2(d), it can be seen that at any investigated pH value, the adsorption capacity of BF on Fe_3O_4@CD is all greater than 23.5 mg/g, and the BF removal rate is all greater than 95%. They change slowly with the increase of pH, suggesting that although pH has a certain influence on the adsorption process of BF on Fe_3O_4@CD, the influence is not obvious. These results also suggest that the proposed adsorption technique can be expected to be developed for the treatment of various kinds of dye wastewater under a wide range of pH. Meanwhile, it can be seen that when pH is 7, the adsorption capacity and removal rate both reach their maximum, indicating that 7 is the optimal pH condition. Therefore, the technique conditions for the adsorption of BF by Fe_3O_4@CD can be optimized as follows: BF initial concentration of 25 mg/L, Fe_3O_4@CD absorbent dosage of 100 mg, at room temperature and at a neutral pH.

3.3 Adsorption mechanism

3.3.1 Adsorption kinetics

The adsorption kinetics of BF on Fe_3O_4@CD was evaluated by using pseudo-first-order, pseudo-second-order and intra-particle diffusion models [39, 40]. Firstly, according to Eqs (3) and (4), the pseudo-first-order and pseudo-second-order kinetic models can be obtained respectively:

$$\ln(q_e - q_t) = \ln q_e - k_1 t \tag{3}$$

$$\frac{t}{q_t} = \frac{1}{k_2 q_e^2} + \frac{1}{q_e} t \tag{4}$$

wherein t (min) is the adsorption time; q_e (mg/g) and q_t (mg/g) are the adsorption capacity at the equilibrium time and at any given time, respectively; k_1 (min^{-1}) and k_2 ($g \cdot mg^{-1} \cdot min^{-1}$) are the reaction rate constants for the pseudo-first-order model or the pseudo-second order one, respectively. According to Eq. (3), the linear plot of $\ln(q_e - q_t)$ versus t gives a straight line as shown in Figure 3(a), where k_1 and q_e for the pseudo-first-order model can be measured from its slope and intercept, respectively. Similarly, according to Eq. (4), the linear plot of t/q_t against t can be obtained as shown in Figure 3(b), where k_2 and q_e for the pseudo-second-order model can also be calculated from the intercept and the slope, respectively.

All parameters of the adsorption of BF dye by Fe_3O_4@CD at different BF initial concentrations for the two kinetic models are presented in Table 1. Obviously, compared with the pseudo-first-order kinetic model, the pseudo-second-order kinetic model has a higher R^2 (greater than 0.9999), indicating that the linear relationship between $\ln(q_e - q_t)$ and t is not as good as that between t/q_t and t. These results disclose that the pseudo-second-order kinetic model can better illustrate the adsorption process of BF dye on Fe_3O_4@CD than the pseudo-first-order one, which can actually be judged from Figure 3 at the same time. Since the rate-determining step of pseudo-second-order adsorption is assumed to be chemisorption-controlled [41], herein, this dominant chemisorption exactly reflects strong electrostatic interactions between cationic BF dye and the Fe_3O_4@CD

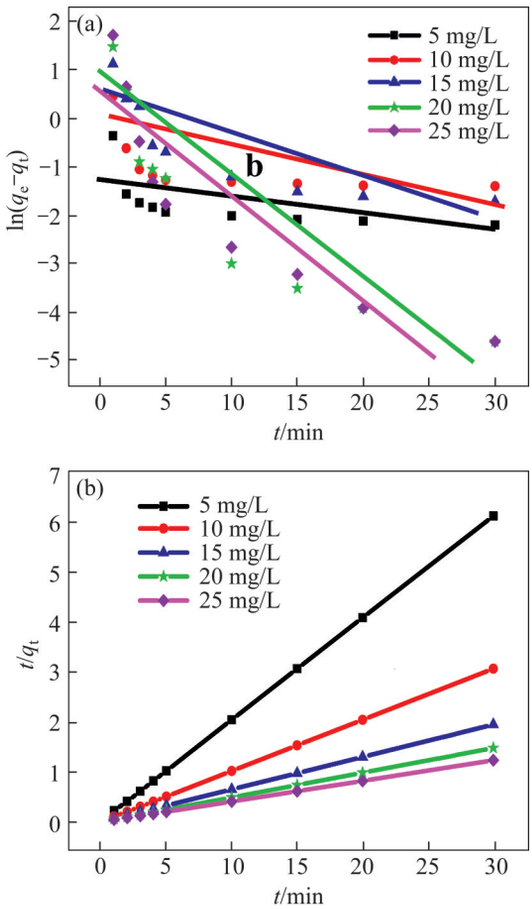

Figure 3 (a) Pseudo-first-order and (b) pseudo-second-order kinetics for the adsorption of BF by Fe_3O_4@CD at different BF initial concentrations ranging from 5 to 25 mg/L (Fe_3O_4@CD 100 mg, room temperature, neutral pH)

absorbent, as described in Scheme 1.

Secondly, in order to further study the adsorption kinetics and the rate-determining step in this adsorption process, the intra-particle diffusion model reported by Weber and Morris can be established according to Eq. (5) [42]:

$$q_t = k_i t^{\frac{1}{2}} + C \quad (5)$$

wherein q_t (mg/g) is the adsorption capacity at time t; k_i (mg·g^{-1}·min$^{-0.5}$) is the intra-particle diffusion rate constant; t (min) is the adsorption time; and C (mg/g) is a constant related to the boundary layer width.

Lines obtained by plotting q_t versus $t^{1/2}$ are shown in Figure 4. According to Weber and Morris, when the plot of q_t to $t^{1/2}$ is a straight line through the origin, the intra-particle diffusion process can be defined as the only rate-determining step [43]. Herein, it is obvious in Figure 4 that the plot of q_t versus $t^{1/2}$ is not a straight line and does not pass through the origin. These results imply that the intra-particle diffusion process is not the only rate-determining step for the adsorption of BF dye by Fe_3O_4@CD. So, there may be other important adsorption processes. Actually, two different linear curves can be seen in Figure 4, suggesting that there are two critical stages involved in the adsorption process. The first stage can be attributed to boundary layer diffusion, in which there is a considerable slop, which reflects that most of BF dye molecules migrate to the boundary layer of the adsorbent Fe_3O_4@CD at a high adsorption rate. The second stage is related to intra-particle diffusion, in which BF dye molecules penetrate into the adsorbent. In this stage, with the gradual saturation of active adsorption sites on the surface of the adsorbent Fe_3O_4@CD, it can be observed that the adsorption rate slows down and the adsorption process reaches equilibrium.

3.3.2 Adsorption isotherms

The adsorption behavior and interaction between the adsorbent and dye molecules can be studied based on common isotherm models, including Langmuir and Freundlich adsorption isotherm models [44].

Table 1 Kinetic model parameters of adsorption of BF by Fe_3O_4@CD at different BF initial concentrations

C_0/(mg·L^{-1})	Pseudo-first-order kinetic model			Pseudo-second-order kinetic model		
	q_{1e}/(mg·g^{-1})	k_1/min^{-1}	R_1^2	q_{2e}/(mg·g^{-1})	k_2/(g·mg^{-1}·min^{-1})	R_2^2
5	4.89	0.034	0.28024	4.90	3.00	0.99992
10	9.75	0.035	0.22570	9.81	1.73	0.99991
15	15.32	0.084	0.64317	15.46	0.34	0.99990
20	20.16	0.189	0.77983	20.29	0.30	0.99998
25	24.16	0.190	0.76254	24.31	0.29	0.99996

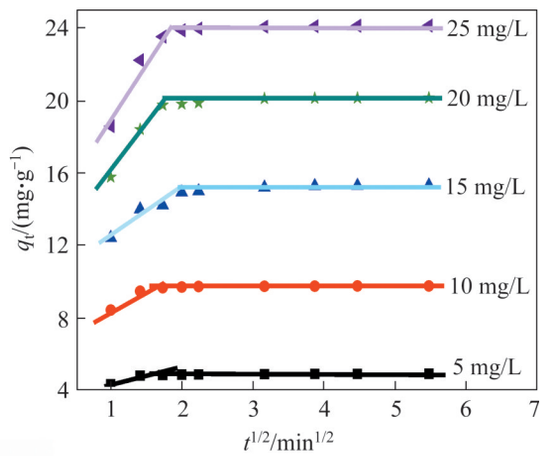

Figure 4 Intra-particle diffusion model for the adsorption of BF dye onto Fe_3O_4@CD magnetic microspheres (BF initial concentration: from 5 mg/L to 25 mg/L; Fe_3O_4@CD: 100 mg; at room temperature; neutral pH)

Langmuir isotherm model assumes that monolayer adsorption occurs at the limited number of adsorption sites on the adsorbent surface. The corresponding parameters can be obtained from Eqs. (6) and (7):

$$\frac{C_e}{q_e} = \frac{C_e}{q_m} + \frac{1}{K_L q_m} \tag{6}$$

$$R_L = \frac{1}{1 + K_L C_0} \tag{7}$$

wherein q_m (mg/g) is the maximum capacity of the adsorbent; C_e (mg/L) is the adsorbent concentration at equilibrium; and K_L (L/mg) is related to adsorption energy, which is called Langmuir binding constant; R_L is used to illustrate the characteristics of adsorption behavior. When the value is 0 − 1, it is favorable for the adsorption; when the value is greater than 1, it is unfavorable for the adsorption. Equal to 1 means reversible adsorption, and equal to 0 means irreversible adsorption [45]. Freundlich isotherm model is based on the assumption that the adsorption heat is not uniformly distributed on the heterogeneous surface. The corresponding parameters can be obtained from Eq. (8):

$$\ln q_e = \ln K_F + \frac{1}{n} \ln C_e \tag{8}$$

wherein q_e (mg/g) is the adsorption capacity at the equilibrium time; K_F is Freundlich constant (related to adsorption capacity); $1/n$ is the heterogeneity factor (related to intensity of adsorption).

All the parameters for both models are summarized in Table 2. It can be seen that R^2 values of Langmuir model are all larger than those of Freundlich model, indicating that Langmuir model can better illustrate this adsorption process than Freundlich model. Thus, the adsorption of BF dye molecules by the Fe_3O_4@CD adsorbent conforms to Langmuir adsorption isotherm, that is to say, monolayer adsorption. Meanwhile, $0<R_L<1$ can be seen from Table 2, which is favorable for the adsorption process. And q_m (mg/g) increases as the temperature rises, which is consistent with the results reported in the previous literature [46].

3.3.3 Thermodynamics

In order to further study the adsorption mechanism of BF dye on Fe_3O_4@CD, the thermodynamics parameters such as free energy change (ΔG^0), enthalpy change (ΔH^0) and entropy change (ΔS^0) have been obtained from Eqs. (9), (10) and (11), respectively [47]:

$$\Delta G^0 = -RT \ln K \tag{9}$$

$$\ln K = \frac{\Delta S^0}{R} - \frac{\Delta H^0}{RT} \tag{10}$$

$$\Delta S^0 = (\Delta H^0 - \Delta G^0)/T \tag{11}$$

Table 2 The adsorption isotherm parameters of the adsorption of BF by Fe_3O_4@CD at different temperature

Temperature/K	Langmuir isotherm model				Freundlich isotherm model		
	R_L	q_m/(mg·g^{-1})	K_L/(L·mg^{-1})	R_1^2	$1/n$	K_F	R_2^2
298.15	0.011	18.67	3.6	0.9979	0.1270	15.98	0.9490
308.15	0.0089	19.45	4.5	0.9990	0.1110	18.17	0.9601
318.15	0.0071	20.57	5.6	0.9995	0.0889	20.05	0.9706
328.15	0.0062	21.55	6.4	0.9999	0.0702	21.02	0.9862
338.15	0.0055	21.91	7.2	0.9999	0.0628	23.00	0.9864

wherein ΔG^0 is the free energy change (kJ·mol^{-1}); R is the gas constant (J·mol^{-1}·K^{-1}); ΔH^0 is the enthalpy change (kJ·mol^{-1}); ΔS^0 is the entropy change (kJ·K^{-1}·mol^{-1}); T (K) is the thermodynamic temperature; K is the equilibrium constant. The values of ΔG^0, ΔH^0 and ΔS^0 can be calculated from the slope and intercept of the van't Hoff plots of ln$K$ versus 1/T (Figure 5), and all of them are listed in Table 3. When ΔG^0 is negative, it indicates that the adsorption of BF dye by Fe_3O_4@CD is spontaneous. According to Ref. [48], the free energy of the physical adsorption process is generally from −20 kJ/mol to 0 kJ/mol, while that of the chemical adsorption process is from −400 kJ/mol to −80 kJ/mol. As can be seen from Table 3, the value range of ΔG^0 in this work is from −17.32 kJ/mol to −21.59 kJ/mol, indicating that the adsorption of BF by Fe_3O_4@CD is not a single physical or chemical adsorption process, but a process of coexistence of both. This is consistent with studies on adsorption kinetics (see Section 3.3.1). Meanwhile, Table 3 shows that the values of ΔS^0 are all positive, suggesting that there is an increase in the randomness at the solid/solution interface during the dye adsorption process. The calculated value of ΔH^0 is 14.80 kJ/mol, implying that the adsorption of BF dye by Fe_3O_4@CD is an endothermic process, that is, the increase in the temperature is conducive to the adsorption.

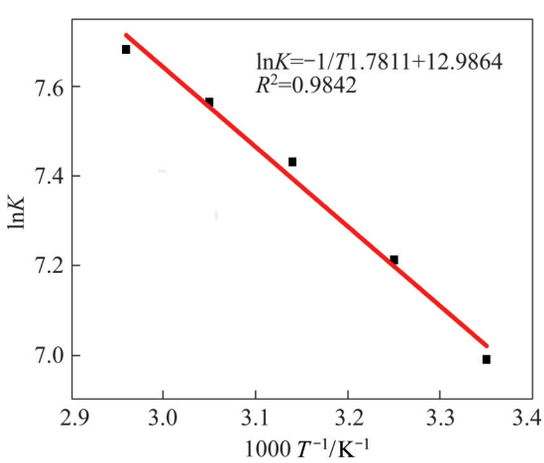

Figure 5 The relationship between ln$K$ and 1/T during the adsorption of BF dye on the Fe_3O_4@CD with the temperature ranging from 25 °C to 65 °C (BF initial concentration 25 mg/L; Fe_3O_4@CD 100 mg, neutral pH)

Table 3 Thermodynamic parameters of the adsorption of BF dye by Fe_3O_4@CD at different temperature

Temperature/ K	ΔG^0/ (kJ·mol^{-1})	ΔH^0/ (kJ·mol^{-1})	ΔS^0/ (J·K^{-1}·mol^{-1})
298.15	−17.32	14.80	107.70
308.15	−18.47	14.80	107.90
318.15	−19.65	14.80	108.30
328.15	−20.63	14.80	107.90
338.15	−21.59	14.80	107.60

3.4 Adsorbent regeneration

The excellent regenerability of adsorbents is of great significance for the treatment of actual dye wastewater. Therefore, the adsorption performance of the prepared Fe_3O_4@CD magnetic microsphere adsorbent was repeatedly investigated 5 times. Figure 6 shows the effect of the regenerated Fe_3O_4@CD absorbent on the removal efficiency of BF dye wastewater. It is clear that the adsorption performance of Fe_3O_4@CD adsorbent toward BF is still good after 5 cycles, with the removal efficiency above 75%. The inset in Figure 6 shows the adsorption-desorption process of BF dye on the Fe_3O_4@CD magnetic microspheres adsorbent. It can be seen from (II) that BF dye in the solution (I) has been adsorbed onto the surface of Fe_3O_4@CD microspheres; from (III), BF dye has been desorbed from the microspheres back into the solution, so that the absorbent Fe_3O_4@CD gets regenerated; from

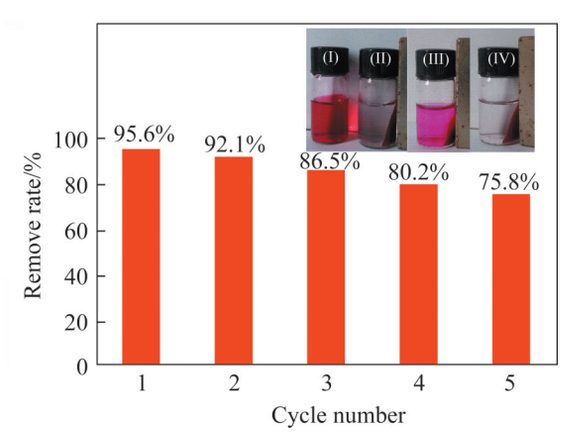

Figure 6 Recycling experiments (The inset: the adsorption−desorption process of BF dye on Fe_3O_4@CD magnetic microsphere adsorbent under an external magnetic field. (BF initial concentration 25 mg/L, Fe_3O_4@CD 100 mg, room temperature, neutral pH): (I) BF dye solution; (II) BF in solution (I) adsorbed by Fe_3O_4@CD; (III) BF desorbed from Fe_3O_4@CD by HCl; (IV) Regenerated Fe_3O_4@CD re-adsorbed BF dye

(IV), BF dye in the solution can be easily re-adsorbed by the regenerated Fe_3O_4@CD. All these results indicate that the recovered Fe_3O_4@CD microspheres not only remain excellent adsorption performance to BF dye pollutants, but also have outstanding magnetic responses to the external magnetic field, which makes its regeneration quite valuable and enables the recycle process fast and convenient enough. Therefore, our prepared Fe_3O_4@CD magnetic microspheres adsorbent has excellent reproducibility and shows a great application prospect in the treatment of industrial dye wastewater.

4 Conclusions

In this work, Fe_3O_4@CD magnetic microspheres have been successfully prepared, with excellent adsorption performances for BF dye. Results show that with 25 mg/L of dye initial concentration and 100 mg of adsorbent dosage under a neutral pH at room temperature, the prepared Fe_3O_4@CD exhibits a best absorption removal effect on BF dye. Further investigations on the adsorption mechanics indicate that the adsorption kinetics is fitted to a pseudo-second order model; the adsorption isotherms are fitted to the Langmuir model with a monolayer-adsorption process; the adsorption thermodynamics are fitted to a spontaneous and endothermic process. Meanwhile, this Fe_3O_4@CD adsorbent shows excellent adsorption performance, strong paramagnetism and good reproducibility after being recycled 5 times. Thus, this easily-regenerated Fe_3O_4@CD absorbent will provide a new economic and eco-friendly way for the treatment of the actual BF dye wastewater.

Contributors

NING Jing-heng designed the experiments and provided financial supports; CHEN Dong-er and HU Qiong-can performed the experiments; LIU Yong-le, HUANG Shou-en, WEI Jia-qian, WEI Rui and SUN Chang analyzed the data and contributed reagents/materials/analysis tools; NING Jing-heng and CHEN Dong-er wrote the paper; WANG Fa-xiang revised the paper; all authors read and approved the final manuscript.

Conflict of interest

NING Jing-heng, CHEN Dong-er, LIU Yong-le, HUANG Shou-en, WANG Fa-xiang, WEI Rui, HU Qiong-can, WEI Jia-qian and SUN Chang declare that they have no conflict of interest.

References

[1] GUPTA V K, MITTAL A, GAJBE V, MITTAL J. Adsorption of basic fuchsin using waste materials-bottom ash and deoiled soya-as adsorbents [J]. Journal of Colloid and Interface Science, 2008, 319(1): 30−39. DOI: 10.1016/j.jcis. 2007.09.091.

[2] WANG Shao-mang, LI Ding-long, SUN Cheng, YANG Shao-gui, GUAN Yuan, HE Huan. Synthesis and characterization of g-C_3N_4/Ag_3VO_4 composites with significantly enhanced visible-light photocatalytic activity for triphenylmethane dye degradation [J]. Applied Catalysis B-Environmental, 2014, 144: 885−892. DOI: 10.1016/j.apcatb.2013.08.008.

[3] PU Hong-yu, TANG Pei-xiao, ZHAO Lu-dan, SUN Qiao-mei, ZHAI Yuan-ming, LI Zhi-qiang, GAN Na, LIU Yuan-yuan, REN Xiu-yun, LI Hui. Preparation of a carboxymethyl beta-cyclodextrin polymer and its rapid adsorption performance for basic fuchsin [J]. RSC Advances, 2020, 10(35): 20905−20914. DOI: 10.1039/c9ra10797e.

[4] BESSASHIA W, BERREDJEM Y, HATTAB Z, BOUOUDINA M. Removal of Basic Fuchsin from water by using mussel powdered eggshell membrane as novel bioadsorbent: Equilibrium, kinetics, and thermodynamic studies [J]. Environmental Research, 2020, 186: 109484. DOI: https://doi.org/10.1016/j.envres.2020.109484.

[5] HUANG Jin, TAN Zhi-qiang, SU Hui-ming, GUO Yi-Wen, LIU Huang, LIAO Bo, LIU Qing-quan. Ferrocenyl building block constructing porous organic polymer for gas capture and methyl violet adsorption [J]. Journal of Central South University, 2020, 27(4): 1247−1261. DOI: 10.1007/s11771-020-4364-4.

[6] CHEN S H, CHEOW Y L, NG S L, TING A S. Biodegradation of triphenylmethane dyes by non-white rot fungus penicillium simplicissimum: Enzymatic and toxicity studies [J]. International Journal of Environmental Research, 2019, 13(2): 273−282. DOI: 10.1007/s41742-019-00171-2.

[7] NAUSHAD M, SHARMA G, ALOTHMAN Z A. Photodegradation of toxic dye using Gum Arabic-crosslinked-poly(acrylamide)/$Ni(OH)_2$/FeOOH nanocomposites hydrogel [J]. Journal of Cleaner Production, 2019, 241: 118263. DOI: https://doi.org/10.1016/jjclepro. 2019.118263.

[8] SHARMA G, KUMAR A, SHARMA S, NAUSHAD M, DHIMAN P, VO D V N , STADLER F J. Fe_3O_4/ZnO/Si_3N_4 nanocomposite based photocatalyst for the degradation of dyes from aqueous solution [J]. Materials Letters, 2020, 278: 128359. DOI: https://doi.org/10.1016/j.matlet.2020. 128359.

[9] PIASKOWSKI K, SWIDERSKA-DABROWSKA R, ZARZYCKI P K. Dye Removal from water and wastewater using various physical, chemical, and biological processes

[J]. Journal of AOAC International, 2018, 101(5): 1371−1384. DOI: 10.5740/jaoacint.18-0051.

[10] JORFI S, BARZEGAR G, AHMADI M, SOLTANI R D C, HAGHIGHIFARD N A, TAKDASTAN A, SAEEDI R, ABTAHI M. Enhanced coagulation-photocatalytic treatment of Acid red 73 dye and real textile wastewater using UVA/synthesized MgO nanoparticles [J]. Journal of Environmental Management, 2016, 177: 111−118. DOI: 10.1016/j.jenvman.2016.04.005.

[11] KHAN Z U H, KHAN A, CHEN Y, KHAN A, SHAH N S, MUHAMMAD N, MURTAZA B, TAHIR K, KHAN F U, WAN P. Photo catalytic applications of gold nanoparticles synthesized by green route and electrochemical degradation of phenolic Azo dyes using AuNPs/GC as modified paste electrode [J]. Journal of Alloys and Compounds, 2017, 725: 869−876. DOI: https://doi.org/10.1016/j.jallcom.2017.07.222.

[12] GUPTA V K, SUHAS. Application of low-cost adsorbents for dye removal—A review [J]. Journal of Environmental Management, 2009, 90(8): 2313 − 2342. DOI: 10.1016/j.jenvman.2008.11.017.

[13] AHMED D N, NAJI L A, FAISAL A A, AL-ANSARI N, NAUSHAD M. Waste foundry sand/MgFe-layered double hydroxides composite material for efficient removal of Congo red dye from aqueous solution [J]. Scientific Reports, 2020, 10(1): 2042. DOI: 10.1038/s41598-020-58866-y.

[14] SHARMA G, ALOTHMAN Z A, KUMAR A, SHARMA S, PONNUSAMY S K, NAUSHAD M. Fabrication and characterization of a nanocomposite hydrogel for combined photocatalytic degradation of a mixture of malachite green and fast green dye [J]. Nanotechnology for Environmental Engineering, 2017, 2(1): 4. DOI: 10.1007/s41204-017-0014-y.

[15] ALBADARIN A B, COLLINS M N, NAUSHAD M, SHIRAZIAN S, WALKER G, MANGWANDI C. Activated lignin-chitosan extruded blends for efficient adsorption of methylene blue [J]. Chemical Engineering Journal, 2017, 307: 264−272. DOI: 10.1016/j.cej.2016.08.089.

[16] WAGN Jie, HOU Guang-ya, WU Lian-kui, CAO Hua-zhen, ZHENG Guo-qu, TANG Yi-ping. A novel adsorbent of three-dimensional ordered macro/mesoporous carbon for removal of malachite green dye [J]. Journal of Central South University, 2020, 27(2): 388−402. DOI: 10.1007/s11771-020-4304-3.

[17] XIA Kai, LIU Xin, CHEN Zhao-jun, FANG Long, DU Hui, ZHANG Xiao-dong. Efficient and sustainable treatment of anionic dye wastewaters using porous cationic diatomite [J]. Journal of the Taiwan Institute of Chemical Engineers, 2020, 113: 8−15. DOI: 10.1016/j.jtice.2020.07.020.

[18] LI Xiao-nan, LI Jing-hua, SHI Wei-lu, BAO Jian-feng, YANG Xian-yuan. A fenton-like nanocatalyst based on easily separated magnetic nanorings for oxidation and degradation of dye pollutant [J]. Materials, 2020, 13(2): 332. DOI: 10.3390/ma13020332.

[19] WU Shui-shen, LAN Dong-hui, ZHANG Xiao-wen, HUANG Yi, DENG Xin-hong, AU Chak-tong, YI Bing. Microwave hydrothermal synthesis, characterization and excellent uranium adsorption properties of $CoFe_2O_4$@rGO nanocomposite [J]. Journal of Central South University, 2021, 28(7): 1955−1965. DOI: 10.1007/s11771-021-4744-4.

[20] GOMEZ-PASTORA J, BRINGAS E, ORTIZ I. Recent progress and future challenges on the use of high performance magnetic nano-adsorbents in environmental applications [J]. Chemical Engineering Journal, 2014, 256: 187−204. DOI: 10.1016/j.cej.2014.06.119.

[21] XU Piao, ZENG Guang-ming, HUANG Dan-lian, FENG Chong-ling, HU Shuang, ZHAO Mei-hua, LAI Cui, WEI Zhen, HUANG Chao, XIE Geng-xin, LIU Zhi-feng. Use of iron oxide nanomaterials in wastewater treatment: A review [J]. Science of the Total Environment, 2012, 424: 1−10. DOI: 10.1016/j.scitotenv.2012.02.023.

[22] FAN Ji-xiang, CHEN Dong-yun, LI Na-jun, XU Qing-feng, LI Hua, HE Jing-hui, LU Jian-mei. Adsorption and biodegradation of dye in wastewater with Fe_3O_4@MIL-100 (Fe) core-shell bio-nanocomposites [J]. Chemosphere, 2018, 191: 315−323. DOI: 10.1016/j.chemosphere.2017.10.042.

[23] JOSHI S, GARG V K, KATARIA N, KADIRVELU K. Applications of Fe_3O_4@AC nanoparticles for dye removal from simulated wastewater [J]. Chemosphere, 2019, 236: 124280. DOI: 10.1016/j.chemosphere.2019.07.011.

[24] CHATTERJEE S, GUHA N, KRISHNAN S, SINGH A K, MATHUR P, RAI D K. Selective and recyclable congo red dye adsorption by spherical Fe_3O_4 nanoparticles functionalized with 1, 2, 4, 5-benzenetetracarboxylic acid [J]. Scientific Reports, 2020, 10(1): 111. DOI: 10.1038/s41598-019-57017-2.

[25] YU Si-yuan, WANG Jin-bao, CUI Jian-lan. Preparation of a novel chitosan-based magnetic adsorbent CTS@SnO_2@Fe_3O_4 for effective treatment of dye wastewater [J]. International Journal of Biological Macromolecules, 2020, 156: 1474−1482. DOI: 10.1016/j.ijbiomac.2019.11.194.

[26] JIN Lin-feng, CHAI Li-yuan, SONG Ting-ting, YANG Wei-chun, WANG Hai-ying. Preparation of magnetic Fe_3O_4@Cu/Ce microspheres for efficient catalytic oxidation co-adsorption of arsenic(III) [J]. Journal of Central South University, 2020, 27(4): 1176−1185. DOI: 10.1007/s11771-020-4358-2.

[27] NING Jing-heng, WANG Yu-fang, WU Qi, ZHANG Xue-feng, LIN Xian-fu, ZHAO Hong-bin. Novel supramolecular assemblies of repulsive DNA-anionic porphyrin complexes based on covalently modified multi-walled carbon nanotubes and cyclodextrins [J]. RSC Advances, 2015, 5(27): 21153−21160. DOI: 10.1039/c4ra15741a.

[28] DUAN Hui-ling, MOU Zhao-li, WANG Jun, MA Shi-yao, ZHAN Han-ying, ZHANG Zhi-qi. Magnetically modified porous β-cyclodextrin polymers for dispersive solid-phase extraction high-performance liquid chromatography analysis of sudan dyes [J]. Food Analytical Methods, 2019, 12(6): 1429−1438. DOI: 10.1007/s12161-019-01476-w.

[29] RAJ V, SARATHI A, CHANDRAKALA T, DHANALAKSHMI S, SUDHA R, RAJASEKARAN K. Guest-host interactions in the alkaline bleaching of triphenylmethane dyes catalysed by β-cyclodextrin [J]. Journal of Chemical Sciences, 2009, 121: 529 − 534. DOI: 10.1007/s12039-009-0064-1.

[30] LIU Jin-shui, LIU Guo-ning, LIU Wen-xiu. Preparation of water-soluble beta-cyclodextrin/poly(acrylic acid)/graphene oxide nanocomposites as new adsorbents to remove cationic dyes from aqueous solutions [J]. Chemical Engineering

Journal, 2014, 257: 299 − 308. DOI: 10.1016/j. cej. 2014. 07.021.

[31] TAKAA L, FOSSO-KANKEU E, PILLAY K, MBIANDA X Y. Metal nanoparticles decorated phosphorylated carbon nanotube/cyclodextrin nanosponge for trichloroethylene and Congo red dye adsorption from wastewater [J]. Journal of Environmental Chemical Engineering, 2020, 8(3): 103602. DOI: 10.1016/j.jece.2019.103602.

[32] LIU Xiao-dong, YAN Liang, YIN Wen-yan, ZHOU Liang-jun, TIAN Gan, SHI Jun-xin, YANG Zhi-yong, XIAO De-bao, GU Zhan-jun, ZHAO Yu-liang. A magnetic graphene hybrid functionalized with beta-cyclodextrins for fast and efficient removal of organic dyes [J]. Journal of Materials Chemistry A, 2014, 2(31): 12296 − 12303. DOI: 10.1039/c4ta00753k.

[33] QU Jian-hua, YUAN Yi-hang, MENG Qing-juan, ZHANG Guang-shan, DENG Feng-xia, WANG Lei, TAO Yue, JIANG Zhao, ZHANG Ying. Simultaneously enhanced removal and stepwise recovery of atrazine and Pb (II) from water using beta-cyclodextrin functionalized cellulose: Characterization, adsorptive performance and mechanism exploration [J]. Journal of Hazardous Materials, 2020, 400: 123142. DOI: 10.1016/j.jhazmat.2020.123142.

[34] LIU Qi-ming, ZHOU Yi, LU Jian, ZHOU Yan-bo. Novel cyclodextrin-based adsorbents for removing pollutants from wastewater: A critical review [J]. Chemosphere, 2020, 241: 125043. DOI: 10.1016/j.chemosphere.2019.125043.

[35] NING Jing-heng, WANG Min, LUO Xin, HU Qiong-can, HOU Rong, CHEN Wei-wei, CHEN Dong-er, WANG Jian-hui, LIU Jun. SiO_2 stabilized magnetic nanoparticles as a highly effective catalyst for the degradation of basic fuchsin in industrial dye wastewaters [J]. Molecules, 2018, 23(10): 2573−2589. DOI: 10.3390/molecules23102573.

[36] ZHU Chun-shan, ZHANG Xiao-yuan, WANG Qiu-ju, ZHANG Rui-li, WANG Ting. Thermo/pH dual responsive beta-cyclodextrin magnetic microspheres for anti-cancer drug controlled release [J]. Journal of Controlled Release, 2015, 213: 21−22. DOI: 10.1016/j.jconrel.2015.05.032.

[37] ZHAN Fang-ke, WANG Ran, YIN Juan-juan, HAN Zeng-sheng, ZHANG Lun, JIAO Ti-feng, ZHOU Jing-xin, ZHANG Le-xin, PENG Qiu-ming. Facile solvothermal preparation of Fe_3O_4-Ag nanocomposite with excellent catalytic performance [J]. RSC Advances, 2019, 9(2): 878 − 883. DOI: 10.1039/c8ra08516a.

[38] MARIAN E, DUTEANU N, VICAS L, RUSU G, JURCA T, MURESAN M, MICLE O, HANGAN A C, STAN R L, IONESCU C, SEVASTRE B, PÁLL E. Synthesis, characterization of inclusion compounds of amygdalin with β-cyclodextrin and sod-like activity and cytotoxicity on hela tumor cells [J]. Arabian Journal of Chemistry, 2020, 13(8): 6828−6837. DOI: 10.1016/j.arabjc.2020.06.035.

[39] HO Y S, OFOMAJA A E. Pseudo-second-order model for lead ion sorption from aqueous solutions onto palm kernel fiber [J]. Journal of Hazardous materials, 2006, 129(1 − 3): 137−142. DOI: 10.1016/j.jhazmat.2005.08.020.

[40] HO Y S. Citation review of Lagergren kinetic rate equation on adsorption reactions [J]. Scientometrics, 2004, 59(1): 171 −177. DOI: 10.1023/B:SCIE.0000013305.99473.cf.

[41] WONG S, TUMARI H H, NGADI N, MOHAMED W B, HASSAN O, MAT R, AMIN N A S. Adsorption of anionic dyes on spent tea leaves modified with polyethyleneimine (PEI-STL) [J]. Journal of Cleaner Production, 2018, 206: 394−406. DOI: 10.1016/jjclepro. 2018.09.201.

[42] LI Xia, NIE Xiao-juan, ZHU Yu-nuo, YE Wen-chao, JIANG Yu-lin, SU Shi-long, YAN Bi-ting. Adsorption behaviour of eriochrome Black T from water onto a cross-linked β-cyclodextrin polymer [J]. Colloids and Surfaces A: Physicochemical and Engineering Aspects, 2019, 578: 123582. DOI: 10.1016/j.colsurfa.2019.123582.

[43] HAI N T, YOU Sheng-jie, HOSSEINI-BANDEGHARAEI A, CHAO Huan-ping. Mistakes and inconsistencies regarding adsorption of contaminants from aqueous solutions: A critical review [J]. Water Research, 2017, 120: 88 − 116. DOI: 10. 1016/j.watres.2017.04.014.

[44] HAGHTALAB A, NABIPOOR M, FARZAD S. Kinetic modeling of the Fischer-Tropsch synthesis in a slurry phase bubble column reactor using Langmuir-Freundlich isotherm [J]. Fuel Processing Technology, 2012, 104: 73 − 79. DOI: 10.1016/j.fuproc.2011.07.005.

[45] LYU Jia-fei, ZHANG Nan, LIU Hong-xu, ZENG Zhou-liang-zi, ZHANG Jing-shuang, BAI Peng, GUO Xiang-hai. Adsorptive removal of boron by zeolitic imidazolate framework: Kinetics, isotherms, thermodynamics, mechanism and recycling [J]. Separation and Purification Technology, 2017, 187: 67 − 75. DOI: 10.1016/j. seppur.2017.05.059.

[46] ZHAO Yong-hua, GENG Jin-tao, CAI Jie-chuan, CAI Yu-fu, CAO Chun-yan. Adsorption performance of basic fuchsin on alkali-activated diatomite [J]. Adsorption Science & Technology, 2020, 38(5): 151 − 167. DOI: 10.1177/02636174 20922084.

[47] RAZMI F A, NGADI N, WONG S, INUWA I M, OPOTU L A. Kinetics, thermodynamics, isotherm and regeneration analysis of chitosan modified pandan adsorbent [J]. Journal of Cleaner Production, 2019, 231: 98 − 109. DOI: 10.1016/j. jclepro.2019.05.228.

[48] LI Qian, YUE Qin-yan, SU Yuan, GAO Bao-yu, SUN Hong-jian. Equilibrium, thermodynamics and process design to minimize adsorbent amount for the adsorption of acid dyes onto cationic polymer-loaded bentonite [J]. Chemical Engineering Journal, 2010, 158(3): 489−497. DOI: 10.1016/j. cej.2010.01.033.

(Edited by YANG Hua)

中文导读

易再生Fe_3O_4@CD磁性微球对碱性品红的高效吸附去除及其吸附机理

摘要：染料废水的过量排放给人类健康和环境带来了严重危害。本文基于β-CD的两亲性和纳米Fe_3O_4的强磁性，制备了磁性吸附剂Fe_3O_4@CD应用于染料废水中碱性品红的高效去除。考察了染料初始浓度、吸附剂用量、温度、pH等系列因素对去除效果的影响及其吸附机理。研究表明，在室温、中性pH值下，当染料初始浓度为25 mg/L、吸附剂用量为100 mg时，所制备的Fe_3O_4@CD对BF的吸附去除效果最佳；其吸附行为符合准二级动力学和Langmuir吸附等温模型，且为自发吸热过程。Fe_3O_4@CD吸附BF后在外加磁场下可快速分离再生，循环使用5次后碱性品红染料去除率保持在75%以上。研究成果有望提供经济环保的实际染料废水处理新技术。

关键词：Fe_3O_4@CD磁性吸附剂；吸附去除；碱性品红